

Evaluation of Pavement Roughness Using an Android-Based Smartphone

Waleed Aleadelat, S.M.ASCE¹; Khaled Ksaibati, Ph.D., P.E.²;
Cameron H. G. Wright, Ph.D., P.E.³; and Promotes Saha, Ph.D., P.E.⁴

Abstract: Modern smartphones are equipped with many useful sensors, such as gyroscopes, magnetometers, global positioning system (GPS) receivers, and three-dimensional (3D) accelerometers. In this study, smartphones' 3D accelerometers were used for collecting a vehicle's vertical acceleration data. Through the use of various signal processing and pattern recognition techniques, such as cross correlations, Welch periodograms, and variance analyses, the measured signals (time series acceleration data) were identified and correlated with the actual international roughness index (IRI) values. It was found that the variance among the vertical acceleration measurements was the key feature for classifying the measured signals. A validation analysis was also conducted to measure the reliability of this methodology. The initial validation results suggested that, using this methodology, the smartphone used could predict with reasonable certainty the actual IRI values. The study was performed on 35 roadway segments extracted from the Wyoming local roads pavement management system (PMS). Also, the selected segments have various lengths and geometric features reflecting the actual roadway segments under any PMS. The major advantage of this technique includes the low-cost solution of measuring local roadway roughness. DOI: 10.1061/JPEODX.0000058. © 2018 American Society of Civil Engineers.

Author keywords: International roughness index (IRI); Smartphone applications; Local roads; Pattern recognition; Accelerometers.

Introduction

According to the US federal law Fixing America's Surface Transportation (FAST) Act, (FHWA 2016), each state is required to develop a pavement management system (PMS). PMS is an assessment tool for decision makers to optimize the allocation of available resources and prioritize the different maintenance and reconstruction projects. Currently, all states have their own PMS. The international roughness index (IRI) is considered a critical pavement condition parameter along with other pavement distresses (Ksaibati et al. 1999). Other pavement distresses include, but are not limited to, pavement condition index (PCI), rut depth, and pavement serviceability index (PSI). The IRI of a roadway segment represents its longitudinal variation of profile, which is a contributor to expected ride quality. A high level of profile variation (i.e., roughness) can also increase vehicle operating cost by 4–5% (Islam and Buttlar 2012). The cost of measuring IRI varies in the range of \$1.40–\$6.20 per kilometer (McGhee 2004). In Wyoming, the cost of collecting roughness and video logs of pavement sections is around

\$31 per kilometer. However, many state department of transportation (DOTs) rely on IRI for their roadways' maintenance and rehabilitation planning (Islam et al. 2014).

In the United States, two-thirds of the roadways' centerline miles are classified as locals, and they carry only 20% of the overall traffic in vehicle miles traveled (VMT) (DOT and FHWA 2011). Hence, many states exclude these local roads from their PMS due to the high costs compared with the traffic volume. However, in Wyoming, the recent industrial/mineral activities on local roads created the need to maintain these roads in acceptable conditions (Aleadelat et al. 2016). Thus, the development of PMS for local road is currently in progress (Saha and Ksaibati 2015). In Wyoming, there are a total of 3,935 centerline kilometers of county paved roads. Developing a PMS requires building a comprehensive maintenance database that includes the different roadway condition indices (i.e., IRI, PCI, and Rut) for each roadway segment. Currently, the state of Wyoming is considering many low-cost approaches for developing PMS for local roads. One approach considers collecting data every two or three years. Another approach is to collect the data for only part of the local roads' network and predicting the remaining part based on the network performance. However, the validity of these approaches is still under investigation (Hafez et al. 2015).

The use of modern smartphones appears to be an appealing approach for reducing the cost of measuring local roads roughness. These smartphones are equipped with many useful sensors such as gyroscopes, global positioning system (GPS), and three-dimensional (3D), or three-axis, accelerometers. In this study, the ability of a smartphone's 3D accelerometer in identifying and estimating local roads' IRI was investigated.

Background

Pavement roughness is the most important factor when it comes to the quality of ride (Carey and Irick 1960). In 1978, Haas and Hudson defined pavement roughness as "distortion of ride quality."

¹Dept. of Civil and Architectural Engineering, Univ. of Wyoming, 1000 E University Ave., Laramie, WY 82070. Email: waleadel@uwyo.edu

²Professor of Civil Engineering, Director of the Wyoming Technology Transfer Center, Dept. of Civil and Architectural Engineering, Univ. of Wyoming, 1000 E University Ave., Laramie, WY 82070. Email: khaled@uwyo.edu

³Professor of Electrical and Computer Engineering, Dept. of Electrical and Computer Engineering, Univ. of Wyoming, 1000 E University Ave., Laramie, WY 82070. Email: chgw@uwyo.edu

⁴Postdoctoral Research Associate, Dept. of Civil and Architectural Engineering, Univ. of Wyoming, 1000 E University Ave., Laramie, WY 82070 (corresponding author). Email: psaha@uwyo.edu

Note. This manuscript was submitted on March 27, 2017; approved on January 17, 2018; published online on June 20, 2018. Discussion period open until November 20, 2018; separate discussions must be submitted for individual papers. This paper is part of the *Journal of Transportation Engineering, Part B: Pavements*, © ASCE, ISSN 2573-5438.

However, pavement roughness includes everything from potholes to the random deviations in a road surface (Gillespie and Sayers 1981). Therefore, it is a result of the interaction between a road surface and the traveling vehicle. ASTM E867-06 (ASTM 2012) defines pavement roughness as “the deviation of a surface from a true planar surface with characteristic dimensions that affect vehicle dynamics and ride quality.”

Pavement roughness affects the level of serviceability that a roadway can provide (Hudson 1981). Thus, pavement roughness is a major contributor to lost-load accidents. In addition, steering control capabilities and friction between the vehicle tire and the road surface are greatly decreased by increased pavement roughness (Burns 1981). Moreover, higher levels of road roughness contribute to decreased roadway capacities and reduced free flow speed (FFS) (Chandra 2004).

As a result, measuring pavement roughness has become a major concern for researchers and highway engineers. A sliding straight-edge (Viagraph) was one of the first fundamental instruments to measure roughness (Gillespie 1992). Due to the difficulty in moving this device, the rolling straightedge device was developed. The rolling straightedge method continued to develop with improvements in the rolling concept. An array of wheels was added to form a reference plane to measure the deviations in the road surface. This type of device represents the early stages of what is now known as a profilograph.

In the 1920s, a vehicle’s vibrations caused by road surface irregularities became a major concern of highway engineers in identifying road roughness. This led to the development of response-type road roughness meters (RTRRMs). These devices measure vertical displacements in the rear axle of a vehicle. One of the major drawbacks of RTRRMs is that they are highly affected by the performance (particularly the suspension) of the vehicle that is used in the measuring process. These devices were not able to provide time-stable measurements. Hence, they were not comparable and not practical to be used for pavement management purposes (Gillespie 1992).

In 1982, the World Bank sponsored a research experiment in order to establish a standard roughness measurement. This research effort resulted in the development of the IRI (Al-Omari and Darter 1994). The IRI is determined by measuring the actual road profile and then processing it through a mathematical algorithm. This algorithm, known as the Quarter Car Simulation, simulates the response of a reference vehicle traveling at 80 km/h (50 mi/h) to road roughness (Gillespie 1992). The accumulated suspension deflections of the reference vehicle can be divided by the traveling distance to provide an index in the units of slope (Shafizadeh and Mannering 2002). Accordingly, IRI is considered a geometric property of the road. Hence, it is a time-stable index, which generates the same values when applied to the same road (Sayers and Karamihas 1995).

The most modern roughness measurement devices are the noncontact profile measuring systems (Islam et al. 2014). These devices measure deviations in longitudinal pavement profile using acoustic or light probes. Then, these measured profiles are processed through Profile Viewing and Analysis (ProVal) software to calculate the IRI. One of the most popular devices of this type is the South Dakota Profiler. This profiler uses two laser sensors to measure the road profile at both wheel paths. The measured IRI is the average IRI of both wheel paths.

Measuring Pavement Roughness Using Smartphone Applications

Modern smartphones are equipped with many useful sensors, such as gyroscopes, magnetometers, GPS receivers, and 3D

accelerometers. These sensors are usually used to identify the orientation of the smartphone screen and other functional activities (Douangphachanh and Oneyama 2013). A 3D accelerometer is a sensor that measures the changes in velocity among the x -, y -, and z -axes in the units of acceleration (m/s^2). Several studies were performed to use 3D accelerometers in identifying roadway conditions (Strazdins et al. 2011; Douangphachanh and Oneyama 2013; Jiménez and Matout 2014; Hanson et al. 2014; Islam et al. 2014). In 2011, Strazdins et al. (2011) performed a study using three Android smartphones to detect potholes and bumps that exist on roadway surfaces. Regardless of the low accuracy of the GPS receivers and 3D accelerometers, they found, using simple algorithms, that the detection of potholes and bumps was possible using smartphones.

In Vientiane, the capital of Laos, Douangphachanh and Oneyama conducted a study to estimate the IRI through smartphone accelerometer measurements (Douangphachanh and Oneyama 2013). They used two Android smartphones (Samsung Galaxy Note II and III) mounted on the dashboard of the test vehicle. Two vehicles, a Toyota VIGO 4WD pickup truck and a Toyota Camry were used in this experiment. The IRI was measured using Vehicle Intelligent Monitoring System (VIMS) for every 100 m (328.08 ft). A Fast Fourier Transform (FFT) was performed on the accelerometer data to obtain a frequency domain view of each signal. A linear relationship was established between the sum of magnitudes from FFT and the measured IRI. The resulting relationship was statistically significant when the speed was less than 60 km/h (37.3 mi/h), with a partial dependence on the vehicle and smartphone types. One year later, Jiménez and Matout (2014) used a tablet’s built in accelerometers to assess the pavement roughness. It was found that the standard deviation of vertical accelerations normalized by the driving speed can give a good indication of the road roughness condition. However, this study did not develop a direct correlation to estimate the IRI; the returned response of the accelerometer was able to identify the different levels of roughness.

In the same year, Islam et al. (2014) conducted a study at the University of Illinois to determine the IRI using a smartphones’ integrated accelerometers. Three test sites (each 3.22 km long) with various roughness conditions were selected. By using a double integration method on the vertical acceleration data obtained by the smartphones, a perceived road profile was formed. The perceived road profile was converted to IRI using ProVAL software. It was found that the calculated IRI values were consistent with the

Table 1. IRI thresholds and descriptions in Wyoming

| IRI (m/km) | Description |
|-------------------|-------------|
| Less than 1.10 | Excellent |
| 1.10–1.56 | Good |
| 1.60–2.05 | Fair |
| 2.07–2.68 | Poor |
| Greater than 2.68 | Very poor |

Table 2. Summary of statistics for the test segments

| Number of test segments | Parameter | Mean | Median | Standard deviation | Maximum | Minimum |
|-------------------------|-------------|------|--------|--------------------|---------|---------|
| 20 | IRI (m/km) | 2.38 | 1.86 | 1.46 | 6.16 | 0.93 |
| | Length (km) | 1.77 | 1.63 | 1.77 | 4.76 | 0.23 |

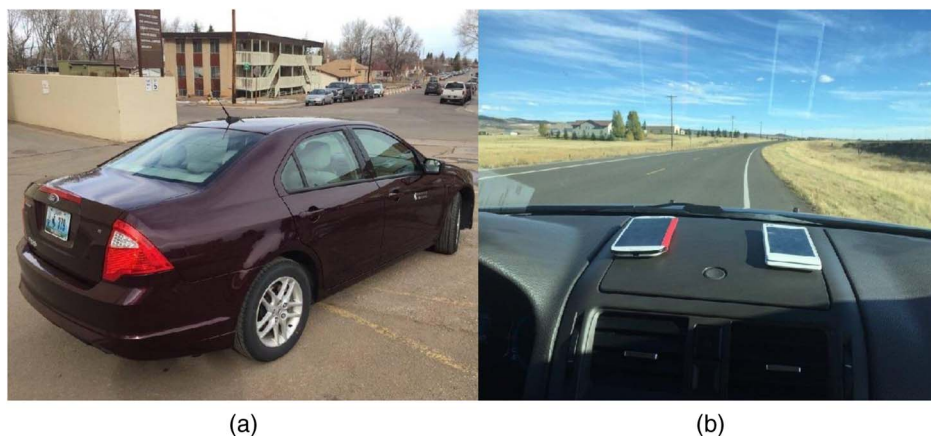


Fig. 1. Test vehicle and smartphone orientation.

measured IRI values using a standard inertial profiler. However, calibration was required for rougher pavement sections to overcome the effect of suspension damping. This methodology was first adapted by Hanson and Cameron in 2012 (Hanson et al. 2014) at the University of New Brunswick, Canada. However, Hanson and Cameron used DATS Toolbox software to convert the acceleration data to displacement. The DATS Toolbox software divides the FFT of the acceleration data by the negative angular frequency of the signal's components squared to get the displacement. This process helps in avoiding the accumulation of errors that result from using numerical integration (i.e., cumtrapz integration).

The preceding studies have documented the smartphones' ability to collect IRI data. However, these studies were limited to measuring IRI at very short test segments with limited changes in horizontal and vertical alignments. Moreover, high pass filters or low pass filters were used to filter the accelerometer data. These filters use certain cutoff frequencies that greatly affect the final calculated IRI values if not used consistently throughout all the measurements. Also, the incorrect selection of cutoff frequencies may eliminate part of the actual frequencies resulting from pavement roughness. Nevertheless, smartphones appear to be a promising tool in minimizing data collection costs, especially at the local level.

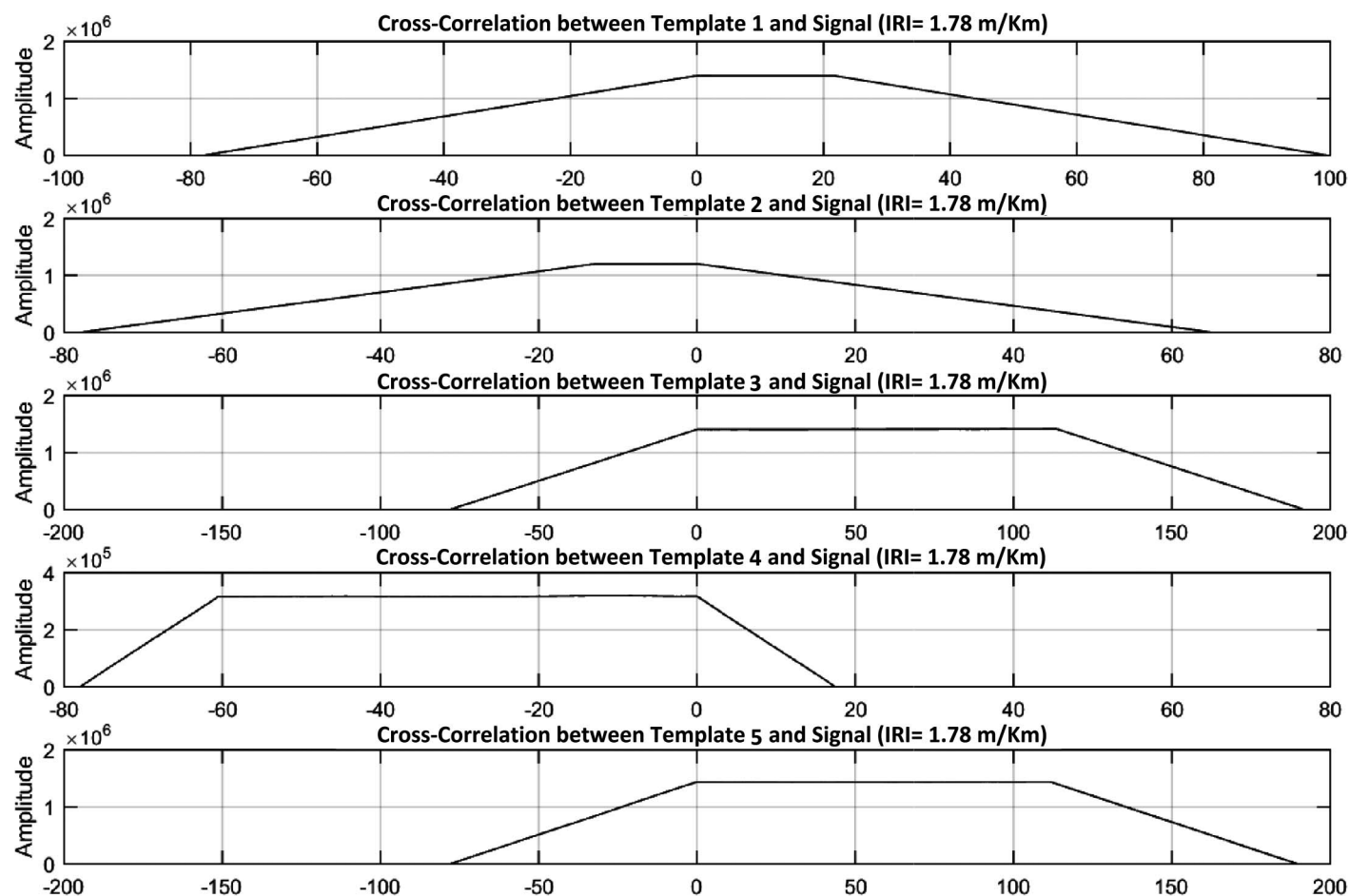


Fig. 2. Crosscorrelation between signal (IRI = 1.78 m/km) and IRI categories (using Samsung Galaxy SIII).

Methodology

This research was based on the idea that roads with similar conditions may provide similar signal patterns (time series acceleration data) using smartphone accelerometers. In other words, smartphone accelerometers were used to capture the vertical vibrations while driving the testing vehicles. Then, different analysis techniques were performed to find the key features among the acquired acceleration signals. Hence, the signals, as produced by the accelerometer, can be considered a reflection of the actual road profile. The following subsections describe this process:

Experiment Design

Two smartphones, a Samsung Galaxy S III and a Sony Xperia A, were selected to collect the vertical acceleration data. The smartphones were glued close to each other on the testing vehicle’s dashboard. A 2011 Ford Fusion sedan was selected as the testing vehicle for this study. Twenty roadway segments were randomly selected from the Wyoming local county roads PMS database for Laramie and Albany Counties. Table 1 shows the different IRI thresholds, according to the Wyoming Department of Transportation (WYDOT), that were considered in this study. The selected segments cover various geometric features with different lengths reflecting the actual roadway segments under any PMS. The referenced roughness measurements were collected using a South Dakota profiler as part of the county roads PMS annual data collection procedure. Table 2 shows a summary of the statistics for the selected test segments.

Data Analysis

Accelerometer data was uploaded to a desktop computer in Microsoft Excel format (*.CSV). Every roadway segment had its own Excel file that represented the variations in speed among the x-, y-, and z-dimensions. Since the smartphones were fixed horizontally (i.e., in x and y), the variations along the z-axis were the focus of this study. Therefore, the time series vertical acceleration data formed a signal that represented the vibrations of the test vehicle, reflecting actual road roughness.

Both median and simple moving average filters were applied to reduce the amount of noise in the accelerometer signals (Mitra 2006). The median filter is a nonlinear digital filter that replaces the neighboring entries of a signal with the median of these entries. The pattern of the neighboring entries is identified by a window that slides over the entire signal. Using this filter helped to eliminate the variations that might be a result of unusual surface anomalies (i.e., potholes and manholes) that can be considered to be statistical outliers. The moving average filter is a digital filter that replaces the neighboring entries of a signal with the average of these entries. This results in reducing the short-term fluctuations and highlighting the longer term trends in the signal. For this study, the acceleration data were filtered first by applying a median filter with a window size of 5. Then, the accelerometer data were filtered again using the moving average filter with a window size of 10. This signal conditioning was accomplished offline as a postprocessing procedure.

Different pattern recognition techniques were used to find similarities or key features between the measured signals at each roughness category. Specifically, crosscorrelation, Welch periodogram

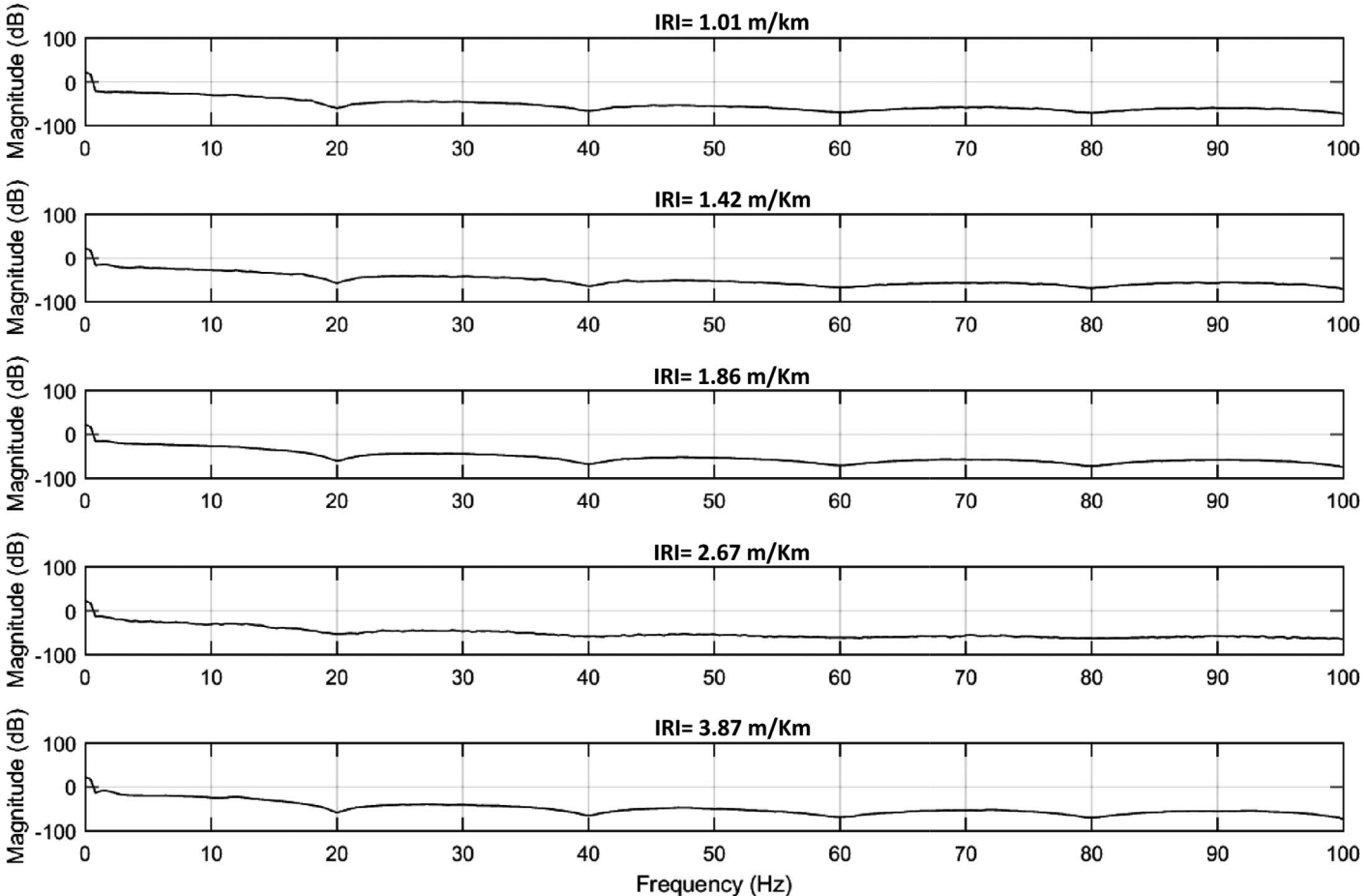


Fig. 3. Welch transformation (using Samsung Galaxy SIII).

estimates of the power spectral density (PSD), and variances among the accelerometer data were performed to recognize the different signals' patterns. The crosscorrelation is a statistical measure of similarity between two different signals. It can be considered to be a sliding dot product of two data series as a function of the lag between the same two series. The crosscorrelation is similar to the mathematical convolution between two functions, except convolution requires one of the two data series to be flipped (i.e., reversed) in time. Autocorrelation is the same procedure as crosscorrelation, except that the two signals are the same signal. In signal analysis, crosscorrelation yields an amplitude function in the units of lag.

The Welch periodogram is a method used to estimate the power in a signal at different frequencies. This is called PSD of a signal. An estimate of the PSD was performed on every measured signal. Then, these estimates were used to identify any unique fluctuations or features of the power among the different frequencies. These fluctuation points can be used as a way to identify the different measured signals.

Finally, variance analysis was conducted to assess the trends of the measured vertical accelerations using the smartphones accelerometers. The calculated variance was compared with the referenced IRI value for each segment. The variance among the accelerometer readings for every segment was calculated as the second central moment according to the following equation:

$$\text{var} = \frac{\sum_{i=1}^n (X_i - \bar{X})^2}{n - 1} \quad (1)$$

where n = total number of vertical acceleration readings for the segment; i = one of the measured vertical acceleration readings

for the segment; X = value for one of the vertical acceleration readings; and \bar{X} = arithmetic mean of the n readings.

This is a well-known method of calculating the unbiased variance of data.

Data Collection

An Android application called AndroSensor was installed on the smartphones that were used in this study. AndroSensor is an application that is used to record data from most of the smartphone sensors. This application is available for free download in the Google Play Store. The application was used to record the smartphone accelerometer data.

Regarding roadway test segments, GPS coordinates of the beginning and ending points were provided as part of the Wyoming local county roads PMS. These coordinates were uploaded into Microsoft Streets and Trips software, which helped in identifying the exact locations of these segments while driving. For every roadway test segment, the smartphone accelerometer data were collected at two velocities; 64 km/h (40 mi/h) and 80 km/h (50 mi/h). The sampling frequency at both velocities was 200 Hz (i.e., 200 samples/s).

As mentioned earlier, the referenced IRI data were collected as part of the PMS using a South Dakota profiler. This device is a laser-type profiler manufactured according to ASTM E950/E950N-09 (ASTM 2018) specifications and meeting Class 1 requirements (Pathway Services 2016). The longitudinal pavement profile for both wheel paths was measured and analyzed using

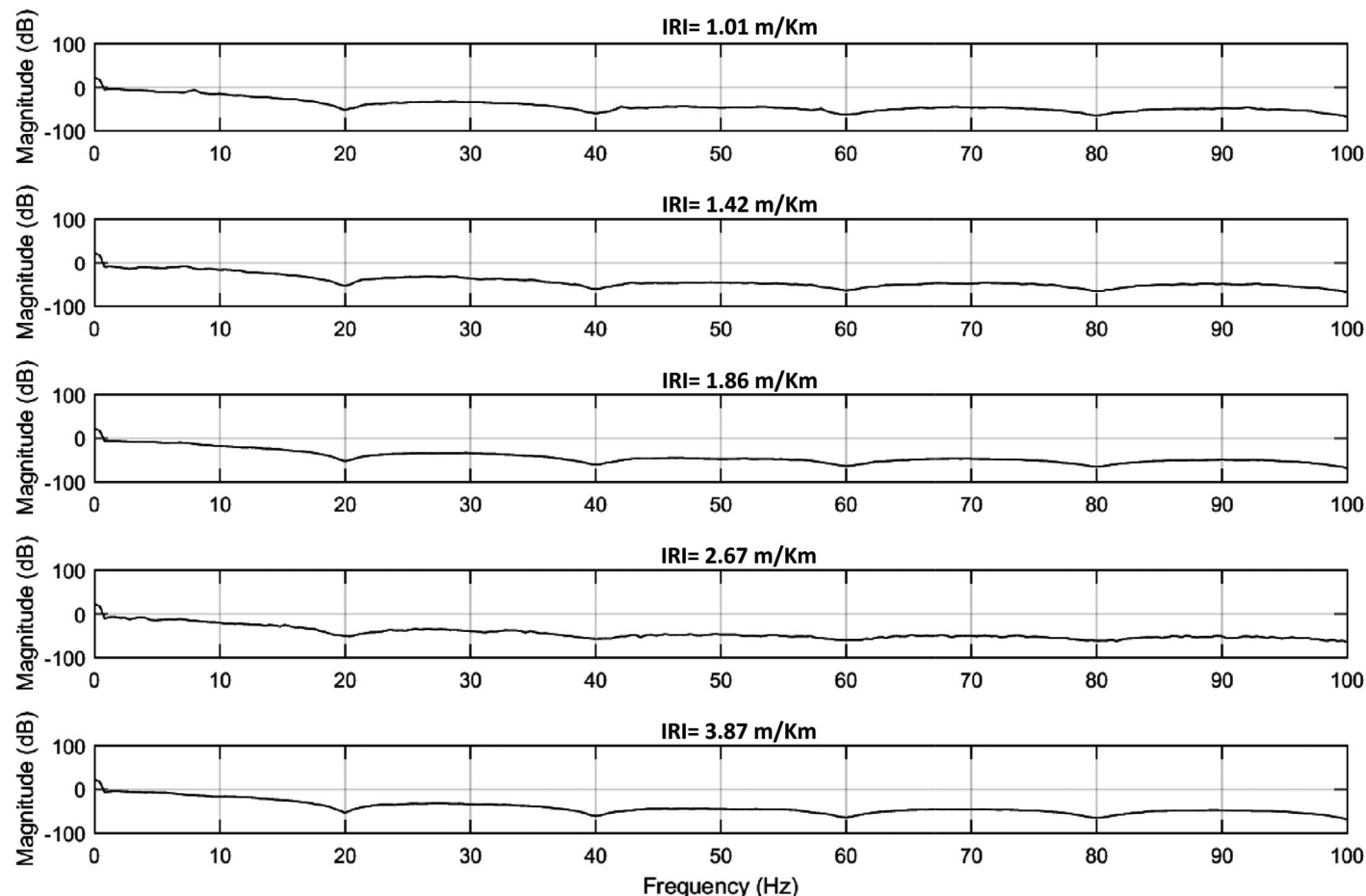


Fig. 4. Welch transformation (using Sony Xperia).

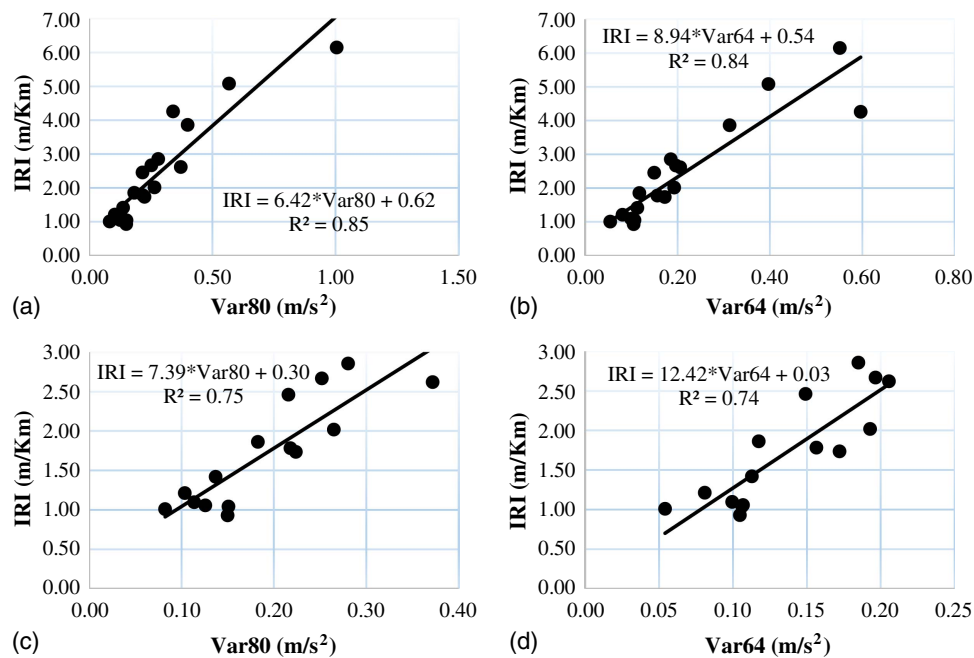


Fig. 5. IRI versus variance (using Samsung Galaxy SIII).

Table 3. IRI thresholds using variances

| IRI (m/km) | var64 (m/s ²) | var80 (m/s ²) |
|-------------------|---------------------------|---------------------------|
| Less than 1.10 | Less than 0.06 | Less than 0.07 |
| 1.10–1.56 | 0.06–0.11 | 0.07–0.15 |
| 1.60–2.05 | 0.12–0.17 | 0.15–0.22 |
| 2.07–2.68 | 0.17–0.24 | 0.23–0.32 |
| Greater than 2.68 | Greater than 0.24 | Greater than 0.32 |

the Quarter Car Simulation to generate the actual IRI value. The average IRI of the right and left wheel paths was considered the final IRI. Fig. 1 shows the test vehicle and smartphone arrangement that were used in this study.

Data Analysis

Accelerometer data was extracted from the smartphones, uploaded to a computer, and imported into MATLAB software for further analysis. After applying median and moving average filters on Samsung Galaxy SIII data, crosscorrelation was applied between the different signals among the various IRI categories. For example, Fig. 2 shows the crosscorrelation between a signal, measured over a roadway segment with IRI = 1.78 m/km at 64 km/h (40 mi/h), and other signals measured within the different IRI categories at the same speed. The crosscorrelation yielded a high amplitude among a wide range of lags over the five IRI categories. This indicates a high similarity in shape between the different measured

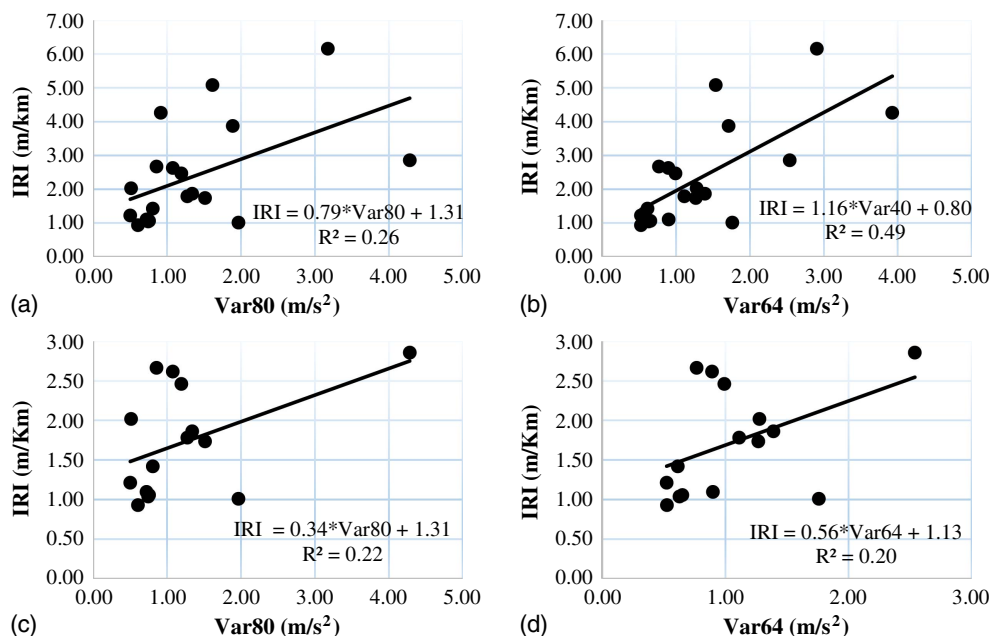


Fig. 6. IRI versus variance (using Sony Xperia).

Table 4. Summary of statistics for the validation segments

| Number of test segments | Parameter | Mean | Median | Standard deviation | Maximum | Minimum |
|-------------------------|-------------|------|--------|--------------------|---------|---------|
| 15 | IRI (m/km) | 2.53 | 1.96 | 1.31 | 5.24 | 0.90 |
| | Length (km) | 2.11 | 1.61 | 2.04 | 8.96 | 0.48 |

signals. Thus, there are no unique features using crosscorrelation that could identify these signals. The same basic result can be seen after applying the crosscorrelation between all 20 measured signals for both speeds. Applying the crosscorrelation analysis on the Sony Xperia data yielded the same results. Roughness does not affect the shape of the produced signals considerably. Thus, the crosscorrelation method did not provide a feature that allowed the desired discrimination between, and classification of, the different IRI categories.

Fig. 3 shows the Welch periodogram estimates of the PSD for different signals measured using the Samsung Galaxy SIII at 80 km/h (50 mi/h). This estimate was calculated using the `pwelch` command of the MATLAB Signal Processing Toolbox, using the default parameters for segments, smoothing window, and overlap. The figure shows that these signals have almost the same PSD trend among the different frequencies. None of these plots show a unique feature that could allow the signals to be used to discriminate between the different IRI categories.

The Welch periodogram estimates of the PSD for the same signals measured using the Sony Xperia are shown in Fig. 4. Again, these signals appear to have a very similar PSD trend without any unique features. Different roughness levels do not seem to have a specific effect on the PSD of these signals. However, the measured signals using both smartphones showed a depression in the signal energy at 20 Hz. This could be attributed to the effect of the vehicle suspension system. Further investigations are required to clarify this trend.

While the previous analyses did not identify useful differences in signal patterns, using variance analysis showed promising results. Figs. 5(a and b) show a significant linear relationship between the referenced IRI and the variance of the vertical accelerometer measurements using the Samsung Galaxy SIII. The variance results can predict with high significance ($R^2 = 0.85$) the referenced IRI values. Also, the results indicate that, as the road roughness increases, the variance among the vertical accelerometer measurements will increase, which is a rational reflection of the actual conditions of the road profile. The same behavior can be observed when using segments with IRI less than 3.16 m/km (200 in./mi) as shown in Figs. 5(c and d).

Using regression analysis, the following two models were developed to predict IRI through smartphone accelerometer measurements:

$$\text{IRI (80 km/h)} = 6.42 \times \text{var80} + 0.62 \quad (R^2 = 0.85) \quad (2)$$

$$\text{IRI (64 km/h)} = 8.94 \times \text{var64} + 0.54 \quad (R^2 = 0.84) \quad (3)$$

where var80 and var64 = variance of the accelerometer readings in m/s^2 (ft/s^2), according to Eq. (1), at 80 km/h (50 mi/h) and 64 km/h (40 mi/h), respectively; and IRI = predicted international roughness index (IRI) in m/km (in./mi).

The driving speed seems to affect the way in which the vehicle responds to the road profile (i.e., variance values). In particular, at 80 km/h (50 mi/h), the variances were higher than those measured at 64 km/h (40 mi/h) for all roadway segments. However, these differences do not detract from the usefulness of the variance to predict the IRI values.

Consequently, solving Eqs. (2) and (3) for the actual IRI thresholds shown in Table 1 yields variance thresholds that can be used to directly identify the measured signals as shown in Table 3. Accordingly, these values can be used directly to classify the roadway segments into the different IRI categories.

Compared with the signals obtained with the Samsung Galaxy SIII, the measured signals using the Sony Xperia showed an insignificant correlation between the referenced IRI and the variance. The variance values were randomly distributed among the different IRI values. In addition, these variance values were considerably higher than the ones obtained using the Samsung Galaxy SIII. This could most likely be attributed to a lower accuracy of the Sony Xperia's accelerometer compared with the Samsung Galaxy SIII. Hence, data from the Sony Xperia in this study could not classify the roadway segments into the different IRI categories. Fig. 6 shows a plot for the variance values versus IRI using the Sony Xperia at 64 km/h (40 mi/h) and 80 km/h (50 mi/h). The same insignificant behavior still holds even after using segments with IRI less than 3.16 m/km (200 in./mi) as shown in Figs. 6(c and d).

Validation of the Models

In order to validate the reliability of the variance models [Eqs. (2) and (3)] in predicting IRI and classifying roadway segments, 15 new segments were selected to perform the experiment again using the Samsung Galaxy SIII. Five of these segments have an IRI greater than 2.68 m/km (170 in./mi). These rough segments were selected to verify the reliability of these models in predicting the IRI of rough segments. Table 4 shows a summary of the statistics for the validation test segments.

Fig. 7 shows the referenced versus the predicted IRI using Eqs. (2) and (3). It can be noted that the variance among the

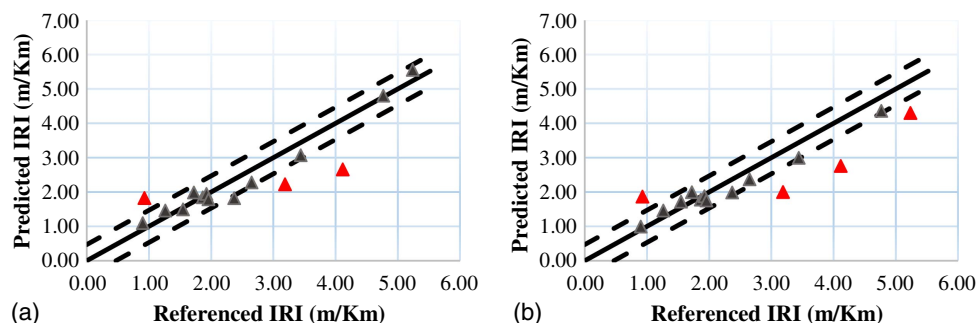
**Fig. 7.** Referenced versus predicted IRI: (a) at 80 km/h; and (b) 64 km/h.

Table 5. *t*-test results

| Test parameter | 80 km/h (50 mi/h) | | 64 km/h (40 mi/h) | |
|------------------------------|-------------------|---------------|-------------------|---------------|
| | Referenced IRI | Predicted IRI | Referenced IRI | Predicted IRI |
| Mean (m/km) | 2.53 | 2.39 | 2.53 | 2.28 |
| Variance (m/km) | 1.84 | 1.53 | 1.84 | 0.92 |
| Observations | 15 | 15 | 15 | 15 |
| Pearson correlation | | 0.91 | | 0.93 |
| Hypothesized mean difference | | 0 | | 0 |
| DF | | 14 | | 14 |
| t Stat | | 0.96 | | 1.62 |
| P(T ≤ t) one-tail | | 0.18 | | 0.06 |
| t critical one-tail | | 1.76 | | 1.76 |
| P(T ≤ t) two-tail | | 0.35 | | 0.13 |
| t critical two-tail | | 2.14 | | 2.14 |

accelerometer data is a promising indicator of the actual roughness level. At 80 km/h (50 mi/h), the predicted IRI of three segments fall outside the 0.47 m/km (30 in./mi) offset band (dashed lines), while four segments fall outside the same band at 64 km/h (40 mi/h). This offset band was set at 0.47 m/km (30 in./mi) because this is the roughness range where a segment moves from a certain IRI category to another (Table 1). In addition, for both speeds, the majority of the rough segments ($IRI > 2.68$ m/km) fall within the offset band. This is because a rougher segment will create more variance within the accelerometer measurements. Hence, using the variance as an explanatory variable to predict IRI can be very helpful in improving the ability of smartphones in identifying rough segments. These segments are highlighted in red (outliers). Nevertheless, the *t*-test results, presented in Table 5, showed that there is no significant difference between the predicted and the measured IRI values at both speeds.

Conclusions

This study demonstrated the capability of smartphone accelerometers for measuring pavement roughness as part of an actual local county roads PMS. Moreover, this study was based on different roadway segments with various geometric features that cover different lengths reflecting the actual roadway segments under any PMS. Using MATLAB, simple signal processing and pattern recognition techniques were applied in order to identify useful features of the different signals measured using smartphones. The features of the signals were compared with referenced IRI values that were measured using a standard profiler (South Dakota profiler). Two models were developed with high correlation to directly predict the IRI through smartphone measurements. The difference between the predicted and the measured IRI was not statistically significant. The main conclusions drawn from this study are as follows:

1. The measured signals (time series acceleration data) using smartphones accelerometers are highly similar in shape. The actual IRI values do not affect the shape of the measured signals meaningfully.
2. Smartphones-measured signals have approximately the same energy at different frequencies (i.e., PSD) within the different IRI levels.
3. The type of the smartphone used seems to be an important factor in measuring the roughness of roadway profiles.
4. Using the Samsung Galaxy SIII, the variance among the vertical accelerometer measurements can, with high certainty,

classify the measured signals within the different IRI categories. However, a few segments were classified outside the designated IRI category.

5. At this stage and using the same combinations of test vehicle and smartphone arrangement, Eqs. (2) and (3) can be used to reasonably predict the actual IRI values. The *t*-test results showed that the difference between the measured and the predicted IRI was not statistically significant.
6. The calculated variance values are speed dependent. However, the speed does not affect the usefulness of variance in predicting IRI. In addition, the variance values were higher at 80 km/h (50 mi/h).

The observed results showed the ability of smartphones in returning acceptable IRI results compared to a standard profiler. These results are compatible with the previous conducted studies in this field. However, the simplicity of data analysis used in this study is very important when it comes to the automation of data collection process. Hence, smartphone applications can be developed easily to return the predicted IRI directly. Nevertheless, further investigations are required to address different variables that may affect the IRI measurement using smartphones. For example, the test could be performed using different types of smartphones, different vehicles, and different lower speeds.

Acknowledgments

This study was supported by the Wyoming Technology Transfer Center (WYT²/LTAP). The authors wish to thank the graduate students Mohammed Okok and Ola Raddaoui for their assistance in collecting the data.

References

- Aleadelat, W., P. Saha, and K. Ksaibati. 2016. "Development of serviceability prediction model for county paved roads." *Int. J. Pavement Eng.* 19 (6): 1–8. <https://doi.org/10.1080/10298436.2016.1176167>.
- Al-Omari, B., and M. I. Darter. 1994. "Relationships between international roughness index and present serviceability rating." *Transp. Res. Rec.* 1435: 132–136.
- ASTM. 2012. *Standard terminology relating to vehicle-pavement systems*. ASTM E867-06. West Conshohocken, PA: ASTM.
- ASTM. 2018. *Standard test method for measuring the longitudinal profile of traveled surfaces with an accelerometer-established inertial profiling*. ASTM E950/E950N-09. West Conshohocken, PA: ASTM.
- Burns, J. C. 1981. "Roughness and roadway safety." *Transp. Res. Rec.* 836: 8–14.
- Carey, W. N., Jr., and P. E. Irick. 1960. "The pavement serviceability performance concept." *Highway Res. Board Bull.* 250: 40–58.
- Chandra, S. 2004. "Effect of road roughness on capacity of two-lane roads." *J. Transp. Eng.* 130 (3): 360–364. [https://doi.org/10.1061/\(ASCE\)0733-947X\(2004\)130:3\(360\)](https://doi.org/10.1061/(ASCE)0733-947X(2004)130:3(360)).
- DOT and FHWA. 2011. "Highway statistics 2009." Table HM-220: Public Road and Street Length, 1980-2009, Miles by Functional Classification. Accessed May 22, 2016. <http://www.fhwa.dot.gov/policyinformation/statistics/2009/hm220.cfm>.
- Douangphachanh, V., and H. Oneyama. 2013. "A study on the use of smartphones for road roughness condition estimation." *J. Eastern Asia Soc. Transp. Stud.* 114: 1551–1564. <https://doi.org/10.11175/easts.10.1551>.
- FHWA (Federal Highway Administration). 2016. "FAST act." Accessed May 22, 2016. <http://www.fhwa.dot.gov/fastact/>.
- Gillespie, T. D. 1992. "Everything you always wanted to know about the IRI, but were afraid to ask!" In *Proc., Road Profile Users Group Meeting*. Ann Arbor, MI: Univ. of Michigan Transportation Research Institute.
- Gillespie, T. D., and M. Sayers. 1981. "Role of road roughness in vehicle ride." *Transp. Res. Rec.* 836: 15–20.

- Haas, R. C. G., and W. R. Hudson. 1978. *Pavement management systems*. New York: McGraw-Hill.
- Hafez, M., K. Ksaibati, and R. Anderson-Sprecher. 2015. "Utilizing statistical techniques in estimating uncollected pavement-condition data." *J. Transp. Eng.* 142 (12): 04016065. [https://doi.org/10.1061/\(ASCE\)TE.1943-5436.0000898](https://doi.org/10.1061/(ASCE)TE.1943-5436.0000898).
- Hanson, T., C. Cameron, and E. Hildebrand. 2014. "Evaluation of low-cost consumer-level mobile phone technology for measuring international roughness index (IRI) values." *Can. J. Civ. Eng.* 41 (9): 819–827. <https://doi.org/10.1139/cjce-2014-0183>.
- Hudson, W. R. 1981. "Road roughness: Its elements and measurements." *Transp. Res. Rec.* 836: 1–7.
- Islam, S., and W. Buttlar. 2012. "Effect of pavement roughness on user costs." *Transp. Res. Rec.* 2285: 47–55. <https://doi.org/10.3141/2285-06>.
- Islam, S., W. G. Buttlar, R. Aldunate, and W. R. Vavrik. 2014. "Measurement of pavement roughness using android-based smartphone application." *Transp. Res. Rec.* 2457: 30–38. <https://doi.org/10.3141/2457-04>.
- Jiménez, L. A., and N. Matout. 2014. "A low cost solution to assess road's roughness surface condition for pavement management." In *Proc., 93rd Annual Meeting of the Transportation Research Board*. Washington, DC: Transportation Research Board.
- Ksaibati, K., R. McNamara, W. Miley, and J. Armaghani. 1999. "Pavement roughness data collection and utilization." *Transp. Res. Rec.* 1655: 86–92. <https://doi.org/10.3141/1655-12>.
- McGhee, K. H. 2004. *NCHRP synthesis 334: Automated pavement distress collection techniques*. Washington, DC: Transportation Research Board of the National Academies.
- Mitra, S. K. 2006. *Digital signal processing: A computer-based approach*. New York: McGraw-Hill.
- Pathway Services. 2016. "Inertial road profiler." Accessed May 20, 2016. http://www.pathwayservices.com/inertial_road_profiler.shtml.
- Saha, P., and K. Ksaibati. 2015. "A risk-based optimisation methodology for pavement management system of county roads." *Int. J. Pavement Eng.* 17 (10): 913–923. <https://doi.org/10.1080/10298436.2015.1065992>.
- Sayers, M. W., and S. M. Karamihas. 1995. *The little book of profiling*. Ann Arbor, MI: Univ. of Michigan Transportation Research Institute.
- Shafizadeh, K., and F. Mannering. 2002. *A statistical analysis of factors associated with driver perceived road roughness on urban highways*. Rep. No. WA-RD 538.1. Olympia, WA: Washington State Dept. of Transportation.
- Strazdins, G., A. Mednis, G. Kanonirs, R. Zviedris, and L. Selavo. 2011. "Towards vehicular sensor networks with android smartphones for road surface monitoring." In *Proc., Second Int. Workshop on Networks of Cooperating Objects (CONET'11): Electronic Proc., CPSWeek'11*, 1–4. Chicago.